Laser Control of Atomic Motion inside Diatomic Molecules

V. M. Akulin,[†] V. A. Dubovitskii,[‡] A. M. Dykhne,[||] and A. G. Rudavets*

Laboratory Aimé Cotton, Bat. 505, Campus d'Orsay, 91405 Orsay, France, Institute of Chemical Physics, 142432 Chernogolovka, Russia, TRINITI, 142092 Troitsk, Russia, and Moscow Institute of Physics and Technology, 141700 Dolgoprudny, Russia

Received: January 6, 1998; In Final Form: March 25, 1998

Globally optimal solution describing a phase conjugated field of Raman scattering on the resonant B ← X transition of iodine I_2 is studied. Maximum optical coherence is found as a top eigenvalue problem. A reversibility theorem has been stated. This provides sufficient conditions for a tightly localized waveform and molecular hologram to exist. A noisy picosecond pulse has been computed to show how femtosecond polarization is regained at target time.

1. Introduction

Molecular wave packet engineering has attracted much attention in the works collected under the rubric of "quantum control".[1−14] Current world-wide efforts in the problematic have been mounted to develop efficient methods for breaking selected molecular bonds[11−14] or to harness specific molecular states for optical processing devices and spectroscopic uses. The rapid progress did not take a long time, because it was prepared by the enormous lore in photomolecular spectroscopy accumulated since Lord Rayleigh epoch and the beginning of quantum mechanics. From the other hand, optimal control theory comprising dynamic programming and modern variational calculus has been the subject of mathematical studies enabling to propose a theoretical apparatus to the quantum control.

Of prime importance were the minimum quantum uncertainty states introduced by Schrödinger. For decades they were meant of only as "Gedankenexperimente". Up-to-date femtosecond technique has made it possible to observe both classically confined states of Rydberg atoms[4] and space-localized wave packets in molecules.[6,9] The title of this paper obliges us to restrict ourselves by the latter. The quantum control theory of ultrafast events close to dissociation limit of diatomic molecules is our major concern. The challenge here is to find optimal laser excitation of picosecond scale causing femtosecond radiation of an optically thin sample.

We shall deal with the subject regarding the iodine I_2 molecule as our test example. Diatomic iodine in gas or condensed state has become the reference standard[15] and ideal benchmark[16,17] in modeling the wave-packet evolution. Our task is greatly facilitated by the considerable volume of researches, in which the quantun control of molecular motion has been exploited theoretically.[5,7,9] The following experiments[6,8,9] with the laser-induced fluorescence (LIF) have supported the idea of wave-packet localization inside a molecule. These works have again emphasized the link of the phase modulated photoexcitation and molecular vibrations, which was broadly known in Raman spectroscopy from 1920s.[18]

The goal yet achieved in the dynamic quantum control[9] includes localization of the vibrational wave packet at the attractive side of molecular potential. This scheme was referred to as the molecular reflectron.[5] Bulk literature has been devoted to focusing the matter states.[3−9] The right posed theoretical limits[10,11] indicate an existence of femtosecond coherence.

Our approach to the problem of a drastical shortening optical transient of a single molecule is started from a crucial relation between a time-reverse molecular dynamics and phase conjugate resonance scattering field. A considerable interest presents a justification of the relation, which, despite its generality, we have not been able to find in the literature. There are two aspects: designing a right chosen objective and tailormaking optimal optical pulses. To understand how they appear, it is worth noting that the rapid improving of femtosecond techniques is based on compression of chirped light pulses provided by the well-established wave guides in optics. One can borrow the key element of the pulse compression physics to apply it to squeezing an optical coherence inside molecular space. Namely, the Franck−Condon region must play a role both dispersive wave guide and frequency modulator owing to molecular vibrations.

The vibrational wave packet is expected to be focused at will on inner Franck−Condon region, since the Franck−Condon factor is at its maximum at the steep repulsive curve. Simultaneously the momentum variance $\Delta p \approx 2M v_0$ will be maximal at this point with v_0 being the wave-packet velocity. The uncertainty principle $\Delta p \Delta q \sim \hbar$ guarantees a tight localization Δq of the rebound wave packet. Thus, its overlap with the ground state, having the variance $\Delta q_0 \gg \Delta q$, lasts just for recoil lifetime ($\sim \Delta q_0/v_0$) and gives rise to ultrashort coherent transient. This picture appeals to the "billard ball" model,[19] which still remains to be extended to involve spreading wave packets on molecular curves. As example we shall look at the reflectron scheme.

The specific iodine reflectron[5,6,9] works at certain frequency above the ground state X. A tailored electric field excites the B state until the wave packet begins to concentrate near an outer turning point far removed from the location of the original Franck−Condon transitions. The closer the excitations to the dissociation limit, the longer a delay before the wave packet will be reflected from the outer curve and moves back to inner repulsive core. From here the wave packet recoils and may

* Corresponding author.
[†] Laboratory Aimé Cotton.
[‡] Institute of Chemical Physics.
[||] TRINITI.

S1089-5639(98)00689-6 CCC: $15.00
Published on Web 05/19/1998

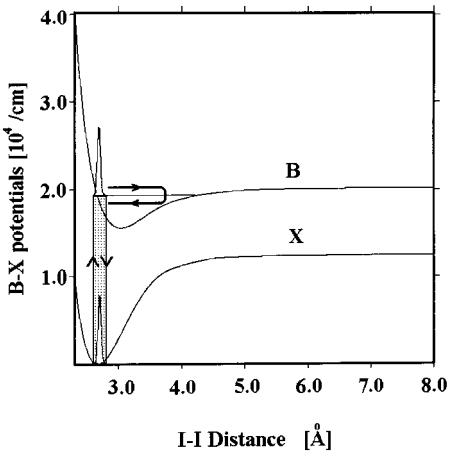

Figure 1. The resonance curves of I_2 molecule.[20] Our design represents the iodine magnetron. A tailored laser pulse, as shown by the point-filled box, excites the vibrational wave packet. Then, the wave packet is reflected from outer curve and moves back to focus on the inner Franck−Condon region. The result is a tight overlap with the ground state X. The maximal optical polarization must be followed by the resonance fluorescence burst at target time.

radiate photons of resonant frequency to the B−X transition, so that an optical coherence begins to appear with a some delay. This "dark" period might cause a fluorescence to spark at a chosen time.

Having the name drawn from the electronic prototype, the molecular reflectron is the scheme to create vibrational wave packet and to focus it on a desired material target. Our prime interest is a radiation process, in which the wave packet is periodically returning into resonance Franck−Condon region and recoiling from it. Hence, a molecular "magnetron" is the best-fitting term to our design, which underlines a parallel between optical−molecular and radio−electronic phenomena. In fact, the vibrational wave packet spreading assisted by molecular anharmonicity could be negated by the tailored laser pulse, because an interplay between its modulation and quantum dispersion squeezes the wave packet, as does a properly chirped radio pulse propagating along a dispersive delay line.

Molecular states promoted nearby their dissociation limit can be localized more tightly than the ground state by itself. For the excited levels are quasiclassical in their nature. Thus, we can treat the recoil lifetime τ_{rec} as a kinematical overlap of the state X and B presented schematically in Figure 1. Here, the resonance Franck−Condon transitions are drawn by the vertical arrows; the horizontal arrows designate the wave packet motion. The wave-packet velocity v and recoil time τ_{rec} are found from the potential functions (molecular curves shown in Figure 1) as

$$v(r) = [2(\epsilon - U_B(r))/M]^{1/2}, \quad \tau_{rec} \approx \int_{R_0}^{R_0+\Delta R} dr/v(r)$$

The distance $R_0 = 2.7$ Å is the equilibrium molecular position in the ground X state of I_2. The ΔR is a maximum variance for the overlapping states, where ϵ is the energy of excitation (equal to an optical frequency) and M is the reduced mass of I_2. The variance $\Delta R = (\hbar/M\Omega)^{1/2} \approx 0.05$ Å (with $\Omega \approx 214$ cm^{-1}) for the ground state is more than it for focused B wave packet on the inner molecular wall. Furthermore, if its variance is disregarded, the recoil lifetime is limited below by the magnitude $\tau_{rec} \approx 15$ fs. The state B can be populated at the energy $\epsilon \approx 19050$ cm^{-1} (∼525 nm) for a more long time than the recoil time τ_{rec}. Setting the gate of excitation by the typical vibrational period $T \approx 546$ fs at ϵ, one can measure the squeezing by the ratio T/τ_{rec} which is expected about 30 or more. As it will be clear later, even subtle details of controlling the atomic motion inside diatomic molecules can be understood by means of the classical characteristics and semiclassical distribution functions.

The plan of our paper is as follows. In section 2 we apply the optimal control theory to optical polarization in the weak field response. A priori pulse shape will not be conjectured. An exact and unique solution to a maximum coherence peaked at target time is derived for isolated I_2 molecule in optically thin media. A time reverse (phase cojugate) resonance Raman scattering providing for a feedback to the vibrational spreading is represented as a basic principle of the quantum control. Controlling the pure and mixed states is considered. In section 3 we reconcile the quantum machinery with a reasoning appealing to the classical kinematics and discuss the phase modulated field of the scattered radiation associated with the classical action of the recoiling wave packet. Section 4 illustrates the general formulation by the numerical simulation. In section 5 we conclude and outline the future prospects.

2. Mapping the Matter to a Light Field

A rigorous mathematical treatment of molecular "magnetron" necessitates to solve the quantum equations dealing on equal footing with vibrational motions and nonadiabatic electronic transitions.

The adiabatic dynamics of a diatomic molecule is governed by Hamiltonian operators $\hat{H}_b = \hat{T}_{kin} + \hat{V}_b$ and $\hat{H}_x = \hat{T}_{kin} + \hat{V}_x$. Here $\hat{T}_{kin}$ is the operator of radial kinetic energy, where the only active coordinate is a distance between atoms, and $\hat{V}_b$ and $\hat{V}_x$ model the adiabatic potentials of the B and X states, respectively. Having the fastest vibrational motion in diatomic molecule, we neglect the more slow molecular rotations (and the fine structure as well), since those transients are separated by time scales.[15] For heavy molecule as I_2, the vibrational transient occurs on a subpicosecond time, while the rotational transient occurs on a longer time scale of 10 ps. Then, we can limit our consideration by the former, because the angular correlations happen past the vibrational ones. In fact, the rotational correction will only require a modification of the Hamiltonians and averaging over initial rovibrational states. As justified in the works,[7,9] the inclusion of the molecular rotations does not abandon the dynamic quantum control of vibrational wave packet toward a desired goal.

Throughout this paper the Condon approximation for dipole transition moment μ is used, with μ being independent of internuclear separation in molecule. This assumption is valid for the weak field quantum control, when the molecular ground state is being well localized. The electronic states are coupled by the electric dipole operator $\hat{V}_{bx}(t) = \hat{\mu}\mathcal{E}(t)$, where the laser field is

$$\mathcal{E}(t) = E(t)e^{i\omega_0 t/\hbar} + \overset{*}{E}(t)e^{-i\omega_0 t/\hbar}$$

and its slow envelop $E(t)$ of allocated duration T_p is to be found under a constrain limiting the pulse energy,

$$J = \int_0^{T_p} d\tau\, E(\tau)\overset{*}{E}(\tau) \qquad (1)$$

This laser field should prepare the molecular transition to a desired goal. Let optical dipole target be a linear superposition of weighted Dirac δ-like envelopes shifted on t_α,

$$G(t) = \sum_{\alpha} G_{\alpha}\delta(t - t_{\alpha}) \tag{2}$$

The wisdom of that representation to the resonance coherence will be obvious further.

The Schrödinger equation for the wave functions Ψ_b and Ψ_x reads as

$$i\hbar\dot{\Psi}_b = (\hat{H}_b - \omega_0)\Psi_b + \hat{V}_{bx}(t)\Psi_x$$

$$i\hbar\dot{\Psi}_x = \hat{H}_x\Psi_x + \hat{V}^{\dagger}_{bx}(t)\Psi_b \tag{3}$$

The empty B state and populated ground X state (at zero temperature) will be of use as our initial condition $\Psi_b(0) = 0$, $\Psi_x(0) = \Psi_{x,0}$. Also, the rotating wave approximation is utilized in eq 3 to avoid fast oscillations of optical frequency of the B−X transition. Then, the resonance interaction is given by the slow amplitude $\hat{V}_{bx}(t) = \hat{\mu}\overset{*}{E}(t)$.

Our objective consists of controlling the polarization

$$D_{xb}(t) = \mu(\Psi^{\dagger}_x|\Psi_b) = \mu\int_0^{\infty} dr\, \overset{*}{\Psi}_x(r,t)\Psi_b(r,t)$$

which in its turn manifests in the molecular optical susceptibility. The first correction to the transition dipole moment $D_{xb}(t)$ in the weak field regime is

$$D_{xb}(t) = -i\int_0^{T_p} d\tau\, S_{00}(t - \tau)\overset{*}{E}(\tau), \quad (t > T_p) \tag{4}$$

To characterize the molecular transition, it is useful to extract a temporal structure factor independing of the excitation field envelope $E(\tau)$. For this goal we introduce a wave-packet correlation function as

$$S_{00}(\tau) = \frac{\mu^2}{\hbar}(\Psi^{\dagger}_{x,0}|e^{-i\tau\hat{H}_b/\hbar}|\Psi_{x,0}) \tag{5}$$

This formula describes the optical polarization caused by the δ-like pulse of electric field $E_s(\tau) = \delta(\tau)$. Modulation of the B−X transitions is formed while the $\Psi_{x,0}$ replica propagates on the B curve. The bound wave packet oscillates spreading between turning points and permits the molecule to radiate the Raman scattering signal. In frequency domain, the erratic spectral pattern[17] of the resonance Raman intensity is accordingly observed. The spectral profile of the S correlator is represented by the KHD formula for the fundamental Raman overtone. Its resonance dependence is given by

$$I_r(\omega) \propto |\int_0^{\infty} d\tau\, e^{i\omega\tau/\hbar}S_{00}(\tau)|^2 = \frac{\mu^4}{\hbar^2}|\sum_m \frac{(\Psi^{\dagger}_{x,0}|\Psi_{b,m})(\Psi^{\dagger}_{b,m}|\Psi_{x,0})}{\gamma + i(\beta_m - \omega)}|^2 \tag{6}$$

where γ is the damping constant; the eigenstates $\Psi_{b,m}$ and eigenleveles β_m can be found from eigenequation $H_b\Psi_{b,m} = \beta_m\Psi_{b,m}$. The Stokes overtones are manifested when the wave packet reaches a favorable position to overlap the vibrational X states.[21]

To maximize the overlap between the Franck−Condon density $|D_{xb}(t)|^2$ and optical dipole target $G(t)$, we define the field functional as

$$F = \int dt\, G(t)|D_{xb}(t)|^2 = \int_0^{T_p} d\tau \int_0^{T_p} d\tau_1\, P_{00}(\tau,\tau_1)E(\tau)\overset{*}{E}(\tau_1) \tag{7}$$

One should note, that given functional does not confine the optical polarization throughout the time. However, it does guarantee a maximal dipole moment at our objective $G(t)$. The Franck−Condon transitions develop freely beyond the target time constrained only by the field energy in eq 1. The dynamic quantum control begins with the X state $\Psi_{x,0}$, which is tightly localized in the I−I distance at the start. The B state must be optimally driven below the dissociation limit to avoid bound-free transitions resulting in losses. Evident wave nature will impede the control, in which the B wave packet having undamped oscillation between turning points, must be focused on the inner steep core with a maximum velocity at target time. Those requirements will be met under a global maximum of the field functional $F/J = \lambda$. This condition is set by small variation of the probe field $\overset{*}{E}(\tau)$ in the variational equation,

$$\delta(F - \lambda J) = 0 \tag{8}$$

where λ is the Langrange multiplier enabling to enforce the energy constrain. Herefrom the basic problem of dynamic quantum control in the weak field regime reduces to the Fredholm eigenequation

$$\int_0^{T_p} d\tau_1\, P_{00}(\tau,\tau_1)\, E(\tau_1) = \lambda E(\tau) \tag{9}$$

where the kernel of the homogeneous equation is given by the complex hermitian matrix

$$P_{00}(\tau,\tau_1) = \int dt\, G(t)S_{00}(t - \tau)\overset{*}{S}_{00}(t - \tau_1) \tag{10}$$

The integral kernel P depends exclusively on a chosen dipole target and specification of the electronic transition being pump independent in the weak field limit. In some sense, it copies the material properties of the molecule to a light field. The time-dependent matrix elements eq 5 forming the kernel in eq 9 have long been known in the "matter-radiation" interaction theory, benefited to understanding nonlinear optics, and were utilized in quantum control of wave packets with different material objectives: the minimum space variance of wave packets (I.S. Averbukh, M. Shapiro[3]), the δ-like space density target (V. Dubov, H. Rabitz[7]), the minimum quantum uncertainty state (K. R. Wilson et al.[5,6,9]).

To recall their argumentation, we shall take a quick look at another field functional, which describes a total B population in the weak field regime

$$N = \int_0^{\infty} dr|\Psi^{(1)}_b(r,t)|^2 = \int_0^{T_p}\int_0^{T_p} d\tau\, d\tau_1\, M_{00}(\tau,\tau_1)E(\tau_1)\overset{*}{E}(\tau) \tag{11}$$

where the self-conjugate kernel $M_{00}(\tau,\tau_1)$ in eq 5 is proportional to the S-correlator depending on the difference argument $\tau - \tau_1$, because the molecular potentials are independent of time

$$M_{00}(\tau,\tau_1) = S_{00}(\tau_1 - \tau)/\hbar = \overset{*}{S}_{00}(\tau - \tau_1)/\hbar \tag{12}$$

Again one can repeat above steps searching a global maximum for the functional $N/J = \lambda$, which gives a maximum population yield per unit field energy. Considering a small field variation $\overset{*}{E}(\tau)$ for the variational equation $\delta(N - \lambda J) = 0$, we obtain an eigenequation

$$\int_0^{T_p} d\tau_1\, \overset{*}{S}_{00}(\tau - \tau_1)E(\tau_1) = \hbar\lambda E(\tau) \tag{13}$$

We obtain the degenerated kernel having separated the time arguments τ and τ_1 by means of the unity decomposition $\sum_m \Psi_{\alpha,m}\Psi^{\dagger}_{\alpha,m} = 1$. Then, a solution to the integral equation can be cast as

$$E(\tau) = \frac{\mu^2}{\lambda_{\max}\hbar^2}\sum_m (\Psi^{\dagger}_{x,0}|\Psi_{b,m})e^{i\beta_m\tau/\hbar}E_m \qquad (14)$$

Unknown coefficients E_m are found from the system of linear equations taken at a maximal eigenvalue $\lambda_{\max}$

$$M_{m,n}E_n = \lambda_{\max}E_m \qquad (15)$$

The matrix $M_{m,n}$ is formed by the Franck−Condon factors and energy levels of the B state

$$M_{m,n} = (\Psi^{\dagger}_{b,m}|\Psi_{x,0})(\Psi^{\dagger}_{x,0}|\Psi_{b,n})\frac{e^{i(\beta_m-\beta_n)T_p/\hbar}-1}{i(\beta_m-\beta_n)} \qquad (16)$$

The optimal field $E(\tau)$ depends on the oscillator strengths of the molecular transition in eq 16, which includes factors of the increasing frequency due to the energy ladder $\beta_0 < \beta_1 ... < \beta_m < ...$ of vibrational levels. This field must steadily populate the molecular states. It is expedient to put on the textbook Condon's model of the molecular transition between the parabolic curve $V_x = M\Omega^2 r^2/2$ and flat continuum $V_b = \text{const}$, where the S-correlator is the following:

$$S_{00}(t) = (1 + i\Omega t/2)^{-1/2} = A_0(t)\, e^{-i\phi_0(t)/2}$$

The phase profile $\phi_0(t) = \arctan(\Omega t/2)$ is provided by the spreading wave packet in continuum which is projected to the ground vibrational state. On using a slope molecular curve, $V_b = -fr$ models the repulsive Franck−Condon region and recoiling wave packet. The phase correction $\phi(t) = \phi_0(t) + t(ft)^2/(12M\hbar)$ is explicitly derived in the model dealing with the momentum representation of wave packet dynamics. The amplitude correction turns out to be of Gaussian type and like the Debye−Waller factor is given by the ratio of the recoil energy $R = (ft)^2/(2M)$ to vibrational quantum $\hbar\Omega$, i.e.

$$A(t) = A_0(t)e^{-R/(2\hbar\Omega)}$$

The flat and slope continuum of molecular states provide for the kernel $S^{*}_{00}(\tau - \tau_1)$ with negative chirp of frequency for a short time duration τ_1, when the expansion in the power of τ_1 is legitimate. The conclusion holds also in a general picture of semiclassical approximation as demonstrated in next section. Thus, a short pulse having positive frequency chirp slows down the fast integrand oscillations in eq 13, enabling one to maximize its eigenvalue (i.e., the yield of the population). The maximum population has to involve a gain of fluorescence.[22−24]

Other trends of wave-packet correlations make it possible to control a selected molecular state or coherent transients. According to eq 9, a top eigenvalue λ gives a maximum optical dipole transition per unit of field energy having eigenvector $E_\lambda(\tau)$ as the globally optimal field of the allocated duration T_p. To demonstrate this statement we address the δ-Dirac model as the simplest optical dipole target, where the coherent envelope $G(t) = \delta(t - t_d)$ will be peaked at time t_d after turning off the excitation pulse. The condition $t_d > T_p$ means that the "spontaneous" polarization will stand out on the pulse-free background. The δ-like target model results in the degenerate Fredholm kernel. An unique solution to the integral equation is explicitly written as

$$E_\lambda(\tau) = S_{00}(t_d - \tau)(J/\lambda)^{1/2} \qquad (17)$$

where t_d marks a moment when the optical polarization is regained with λ being the normalized coherent yield

$$\lambda = \int_0^{T_p} d\tau\, S_{00}(t_d - \tau)S_{00}(t_d - \tau) \qquad (18)$$

The indication of optimality according to Bellman principle is indeed realized: the control depends on the state of system at the current moment alone. This globally optimal fields can be understood in general terms, for their envelopes $E_\lambda(\tau)$ match those of the wave packet correlations representing the time-reversed resonance scattering. The delay time t_d fits an absolute maximum of the optical transient to target time $\tau = t_d$. The dipole transition moment is given by the convolution integral

$$D_{xb}(t) = -i(J/\lambda)^{1/2}\int_0^{T_p} d\tau\, S_{00}(t - \tau)\, S^{*}_{00}(t_d - \tau) \qquad (19)$$

The optimal field in eqs 17 and 19 cancels out the fast oscillating behavior of the integrand as being designed to have the phase conjugate wave-packet correlations excited by the δ-like pulse. The optical transient by virtue of eq 19 exhibits periodical recurrences, having the maximum magnitude $-i(J\lambda)^{1/2}$ exactly at the target time t_d.

The straightforward extension of the δ -dipole target to the realistic shape $G(t)$ specifies an eigenvalue problem in eq 9. The integral operator P can be decomposed into sum of the degenerate kernels according to eq 10 in the weak field limit. The solution is

$$E(\tau) = \sum_\alpha S_{00}(t_\alpha - \tau)G_\alpha E_\alpha/\lambda_{\max} \qquad (20)$$

where the E_α is the eigenstate at a top eigenvalue of the system

$$\hat{P}_{\alpha\alpha_1}E_{\alpha_1} = \lambda_{\max}E_\alpha \qquad (21)$$

The matrix coefficients are given by

$$\hat{P}_{\alpha\alpha_1} = G_\alpha\int_0^{T_p} d\tau\, S_{00}(t_\alpha - \tau)\, S^{*}_{00}(t_{\alpha_1} - \tau) \qquad (22)$$

so that the optimal field satisfies the energy constrain by the definition.

We have established an important fact, which merits to be reformulated as a reversibility theorem asserting sufficient conditions to reverse the spread wave packet in time: *To drive molecular transition to the polarization target G(t), the optimal field should be made of superimposed phase conjugate fields of the resonance Raman scattering of ultrashort pulses of amplitudes $G_\alpha E_\alpha/\lambda_{\max}$ at the delay time t_α.*

The resonance scattering radiation itself may seem to be "erratic" in time. The wave-packet collapse and spreading and destructive interference are responsible for the apparent noise due to molecular "disorder" on account of potential anharmonicity, uncommensurate frequencies, curve crossing, etc. But phase conjugate feedback with respect to molecular correlations (resonant scattering) allows the wave packet to be recovered at a fixed space−time point at will. The optical coherence can be restored not only for the Raman fundamental overtone. Our treatment might be readly extended to controlling the high overtones of molecular resonance scattering.

We term the field enabling to squeeze the optical coherence as a quantum hologram to note its key role for a wave-packet interference in the Franck−Condon region. The quantum holography is relying on the wave-packet correlations, which can be found by detecting a fluorescence or population created by two-phase locked ultrashort pulses. Accordingly, in the limit of weak field, the excited-state B is obtained from eq 3, in the first order to the resonance interaction as

$$\hat{\Psi}_b^{(1)}(t) = -i\theta_1 e^{-it\hat{H}_b/\hbar}\hat{\Psi}_{x,0}(0) - i\theta_2 e^{-i(t-T)\hat{H}_b/\hbar}\hat{\Psi}_{x,0}(T) \quad (23)$$

This superposition is obvious analogue of an incident and object waves in optical holography. To produce the quantum interference of wave packets, the first laser pulse at $t = 0$ must be followed by the delayed pulse at $t = T$. If the laser pulses are phase locked and their areas are small with respect to π, the population N of the state B contains the contribution[14] of the one-photon two-pulse interference, i.e.,

$$N = \int_0^\infty dr|\Psi_b^{(1)}(r,t)|^2 = |\theta_1|^2 + |\theta_2|^2 + Re\left\{\theta_2 \overset{*}{\theta}_1 S_{00}(T)\right\} \quad (24)$$

The alternative pathways in course of the Franck−Condon transitions depend on the delay time T between pulses. This dependence is being just required to controlling the wave-packet motion. The phase-locked laser pulses must retrieve synphase and quadrature components of the S correlator. The LIF signal,[14] ionization channel,[25] or other means for the matter−wave interferometry may be employed. Then, the use of programmable optics[26,27] and algorithms based on the reversibility theorem fed into computer codes can be made to tailor the optimal field. This quantum holography program must be realized to rebuild the well-localized replica of the ground state or to squeeze optical coherence as called on even for unknown molecular curves as well as collisional or intramolecular dephasing and relaxation.

The reversibility theorem still holds for mixed states inevitably residing in statistical systems, for which irreversible processes hamper the quantum control of the wave packets. By considering the nondiagonal density matrix of the resonance transition $\hat{\rho}_{\alpha\beta} = \langle\hat{\Psi}_\alpha^\dagger\hat{\Psi}_\beta\rangle$, the brackets $\langle ...\rangle$ symbolize an ensemble averaging in quantum kinetic theory. Here, the populations $\hat{\rho}_{xx} = \langle\hat{\Psi}_x^\dagger\hat{\Psi}_x\rangle$, $\hat{\rho}_{bb} = \langle\hat{\Psi}_b^\dagger\hat{\Psi}_b\rangle$ and polarization $\hat{\rho}_{bx} = \langle\hat{\Psi}_b^\dagger\hat{\Psi}_x\rangle$ adhere to the kinetic equations:

$$i\hbar\frac{\partial\hat{\rho}}{\partial t} = [\hat{H},\hat{\rho}] - i(\hat{\Gamma}\hat{\rho}) \quad (25)$$

where the rectangular brackets [...] denote a quantum commutator $\hat{H},\hat{\rho} - \hat{\rho},\hat{H}$ of the operators which are represented in the matrix notation as

$$\hat{\rho} = \begin{pmatrix}\hat{\rho}_{bb}, \hat{\rho}_{bx}\\ \hat{\rho}_{xb,}\ \hat{\rho}_{xx}\end{pmatrix}, \quad \hat{H} = \begin{pmatrix}\hat{H}_{bb}, \hat{V}_{bx}\\ \hat{V}_{xb}, \hat{H}_{xx}\end{pmatrix} \quad (26)$$

A phenomelogical damping matrix $\hat{\Gamma}$ designates the overall losses in irreversible processes for collisions, spontaneous radiation, etc. Experiments in solids, liquids, and gas cell conditions indicate an existences of coherent vibrational transients of I_2 to tens of picoseconds.[14] Thus, the quantum control theory within the matrix density formalism, in which the relaxation will not be scrutinized further, may be applied.

Just as for pure states, we take care of the optical polarization $\hat{\rho}_{bx}$ at target time. One can immediately maximize the overlap between the optical transition ρ_{bx} and its dipole target in eq 2. By letting the polarization operator $\hat{\rho}_{bx}$ be a complex valued quantity, we define an overlap functional as

$$F = -\mu\int dt\, Im\{G(t)\, Tr\{\hat{\rho}_{bx}\}\} = \int_0^{T_p} d\tau\, Re\left\{\overset{*}{E}(\tau)P_{00}(\tau)\right\} \quad (27)$$

where another field functional $P_{00}(\tau)\}$ is easily obtained from eqs 25 and 26 to be

$$P_{00}(\tau) = \frac{\mu^2}{\hbar}\int dt\, G(t)\, e^{-\Gamma(t-\tau)}\, Tr\,\{e^{-i(t-\tau)\hat{H}_b/\hbar}\,[\hat{\rho}_{xx} - \hat{\rho}_{bb}]\, e^{i(t-\tau)\hat{H}_x/\hbar}\} \quad (28)$$

The functional F is indentified as a work that a given target $G(t)$ would produce on the Franck−Condon transition. This statement can be readily understood, since according to eq 25 the field functional F can be rewritten as the populations difference due to the target field "action"

$$F = -\int dt\, ImTr[G(t)\hat{\rho}_{bx}(t)] = \hbar\int dt\, Tr[\dot{\hat{\rho}}_b(t) - \dot{\hat{\rho}}_x(t)] = \hbar(N_b - N_x)$$

To maximize F, we apply the standard variational procedure of eq 8. The dynamic quantum control in the weak field limit reduces to a problem of a linear mathematical programming. As a bonus of the approach, no integral equation needs to be solved at all, because, even for any target shape $G(t)$, the variational equation

$$\delta(F - \lambda J)/\delta\overset{*}{E}(\tau) = 0$$

results in an unique solution:

$$E(\tau) = \lambda^{-1}P_{00}(\tau) \quad (29)$$

By using the empty B state and populated state X, $\hat{\rho}_{bb} = 0$ $\hat{\rho}_{xx} = \hat{\rho}_0$, as the initial conditions, we set that

$$P_{00}(\tau) = \frac{\mu^2}{\hbar}\int dt\, G(t)e^{-\Gamma(t-\tau)}Tr\{e^{-i(t-\tau)\hat{H}_b/\hbar}\hat{\rho}_0 e^{i(t-\tau)\hat{H}_x}\} \quad (30)$$

and the maximum coherent yield λ becomes explicitly known from the energy constrain represented as

$$\lambda^2 = J^{-1}\int_0^{T_p}\overset{*}{P}_{00}(\tau)P_{00}(\tau)d\tau \quad (31)$$

By choosing the pure state $\hat{\rho}_0 = \Psi_{x,0}^\dagger\Psi_{x,o}$ for the initial condition, we recover the main result of eq 5, as it must. Matrix density formulation has the advantage of being applied to irreversible physical systems of gas and condensed matter. The predissociation[47] and caging phenomena can be considered as well. What is more, the observation and control of wave packets is in the progress[8,9] and includes rearrangement of subtle chemical structures in solids and liquids. Having postponed the feasible generalization, we shall discuss in next section the reversibility theorem in the semiclassical uniform approach.

3. Semiclassical Approximation

The semiclassical limit of quantum dynamics is characterized by classical equations, that require to be supplemented by the quantum initial conditions to take full account of the singularity

$\hbar = 0$. The former is clear, only classically possible paths joining R_0 with R_1 contribute to the S-correlator. These paths are invoked by Hamilton's principle $\delta W = 0$, where the classical action is

$$W(R_0,R_1,t) = \int_0^t \mathrm{d}\tau\left(\frac{M}{2}\dot{R}^2(\tau) - U_\mathrm{b}(R(\tau))\right) \qquad (32)$$

If the action is known, it enables us to find a momentum $P_0 = -\partial W(R_0,R_1,t)/\partial R_0$ and density of states $\partial P_0/\partial R_1$. Appearance of the derivative of classical trajectory in determining the density distribution in phase space is not occasional.[28] The quantum transition amplitude connecting the points R_0 and R_1 depends on Plank's constant $\hbar$ and cannot be deduced from the classical postulate. Instead, the quantum grounds dictate

$$K(R_0,R_1,t) = \langle R_0|\mathrm{e}^{-\mathrm{i}tH_\mathrm{b}/\hbar}|R_1\rangle = (-2\mathrm{i}\pi\hbar\delta R_1/\delta P_0)^{-1/2}\exp(\mathrm{i}W(R_0,R_1,t)/\hbar) \qquad (33)$$

The probability density, $|K|^2 = (2\pi\hbar)^{-1}\delta P_0/\delta R_1$, stems from the total number of atoms reached the point δR_1 started out from the point R_0 and having the classical action $W = W(R_0,R_1,t)$. Equation 33 does not give the quantum amplitudes correctly for certain space−time points. Suffering from known drawbacks, it fails in the classically forbidden region, caustics, and turning points. The story is old as the quantum theory itself. However, for our goals, the semiclassical approach does at least serve to a clue idea about the quantum control.[29]

The classical action W is inherited by the phase of electric field promoting resonant B−X transition. By this, the optimal laser field is related with the S-correlator which projects the wave packet B to the ground-state X. The latter is centered at $R_0 = 2.7$ Å in the I−I distances with the variance $\Delta R = 0.05$ Å being much less than the Franck−Condon region extension itself. Hence, the mere closed paths passing the point R_0 contribute to the optimal field. We can present its phase by the classical action eq 33 expanded for ultrashort pulse as

$$W(R_0,R_0,t_\mathrm{d}-\tau) = W(R_0,R_0,t_\mathrm{d}) + U_\mathrm{b}(R_0)\tau - M(\ddot{R}_0)^2\tau^3/3 \qquad (34)$$

in the vicinity of inner turning point R_0. The potential $U_\mathrm{b}(R_0)$ plays the role of frequency detuning of the B−X transition. Owing to zero velocity $\dot{R}_0 = 0$, its linear chirp will be negligible as compared with the nonlinear chirping. Instead, there is a significant quadratic chirp $-M(\ddot{R}_0)^2\tau^2 t$ as adominant feature of acceleration $\ddot{R} = -M^{-1}(\mathrm{d}U_\mathrm{b}(R)/\mathrm{d}R)$ due to the steep inner core. By travelling a distance δr in vicinity of R_0, the wave packet detunes down the resonant frequency on $\delta r(\mathrm{d}U_\mathrm{b}(R)/\mathrm{d}R)$. The greater $\delta r = \ddot{R}_0\tau^2$ the smaller the frequency of B−X transition. This gives the negative chirp, which qualitatively is in agreement with the known reasoning.[6,29] In practice, for a more longer pulse duration, this simple classical expression may overestimate the chirp rate, because the particle also travels far from the steep potential in a less repulsive Franck−Condon region. Reduction of frequency modulation, as well as linear chirping owing to a wave packet velocity, is quite possible.

Care must be taken to the turning points, where the semiclassical transition amplitude postulated in eq 33 diverges $\partial R_1/\partial P_0 = 0$. This is the case for our molecular magnetron design, in which the wave packet must be focused just in vicinity of the inner turning point. This severity can be circumvented by the uniform approach based on the Wigner representation of quantum operators. To find the S-correlator density, we must overlap the initial and propagated distributions in the phase space $s = (r,p)$,

$$|S(t)|^2 = \frac{\mu^4}{\hbar^2}\int_s \mathrm{d}r\,\mathrm{d}p\;\rho_0(r,p)\rho_0(R,P) \qquad (35)$$

where $R = R(-t;\, s,\, 0)$ and $P = P(-t;\, s,\, 0)$ being the current coordinate and momentum of a particle experiencing the force $-\partial U_\mathrm{b}(R)/\partial R$. The classical integrals of motion are fixed by the initial conditions $R(0;\, s,\, 0) = r$ and $P(0;\, s,\, 0) = p$ in the phase space. According to the Newton laws, the particle travels as

$$\dot{R} = P/M \qquad P = -\partial U_\mathrm{b}(R)/\partial R \qquad (36)$$

and the Wigner density function obeys the transport equation:

$$\frac{\partial\rho_0(s,t)}{\partial t} + \frac{p}{M}\frac{\partial\rho_0(s,t)}{\partial r} - \frac{\partial U_\mathrm{b}(r)}{\partial r}\frac{\partial\rho_0(s,t)}{\partial p} = 0 \qquad (37)$$

Hence, the solution is $\rho_0(R(0;\, s,\, t),\, P(0;\, s,\, t))$ propagating along the trajectory passing the point s in time t with the distribution for the ground X state, which is defined as

$$\rho_0(r,p) = \int_{-\infty}^{\infty}\frac{\mathrm{d}q}{2\pi\hbar}\mathrm{e}^{\mathrm{i}qp/\hbar}\Psi_{\mathrm{x},0}^{\dagger}\left(r+\frac{q}{2}\right)\Psi_{\mathrm{x},0}\left(r-\frac{q}{2}\right) = \frac{1}{\pi\hbar}\mathrm{e}^{-F(p,r)} \qquad (38)$$

where

$$F(p,r) = ((r - R_0)/\Delta R)^2 + (p\Delta R/\hbar)^2 \qquad (39)$$

The Wigner function of the ground state X is sharply peaked at the point $q_0 = (R_0,0)$ having Gaussian variances $(\Delta R,\hbar/\Delta R)$ in the coordinates and momenta, respectively. The classical orbits passing this stretched ellipse make a major contribution to the S-correlator amplitude.[48] Then, one can apply the fastest descent method to estimate the amplitude in eq 35. We expand the exponent functional $F(R,P)$ to second order in the declines from the path $s_0(t) = (R(0;q_0,t),\, (P(0;q_0,t))$ passing the equilibrium point q_0 of the ground X state. The family of orbits in its neighborhood contributes significantly. Thus, this topology determines basically a quadratic form

$$F(R,P) = F^0 + F_s^0(s - q_0) + \frac{1}{2}F_{s,s_1}^0(s - q_0)(s_1 - q_0) + \ldots \qquad (40)$$

The function $F^0 = F(s_0(t))$ is taken on the path $s_0(t)$. A small stirring of its initial condition yields the four first and six second derivatives of R and P with respect to two-dimensional indices $s = (r,p)$ or $s_1 = (r,p)$. Then, the quadratic form is settled by the 12 related functions:

$$R(0;q_0,t),\quad P(0;q_0,t),\quad R_s(0;q_0,t),\quad P_s(0;q_0,t),\quad R_{s,s_1}(0;q_0,t),\quad P_{s,s_1}(0;q_0,t)$$

Of course, these functions adhere to Newton's equations and their derivatives. The useful vector and matrix notations

$$\vec{V} = (F_r^0,\, F_p^0);\ \hat{F} = \begin{pmatrix}(\Delta R)^{-2} + F_{rr}^0/2, & F_{\mathrm{rp}}^0\\ F_{rp}^0, & (\Delta R/\hbar)^2 + F_{pp}^0/2\end{pmatrix} \qquad (41)$$

simplify the resulting Gaussian integral:

$$|S(t)|^2 \propto \hbar^{-1}(\det\hat{F})^{-1/2}\exp(-F^0 + {}^1/_4\vec{V}\hat{F}^{-1}\vec{V}^{\dagger}) \qquad (42)$$

The derivatives of the classical path with respect to its starting point in the space s represent the states density already mentioned in this section. Now we see that a given method

leads to the determinant in denomenator to set a density of paths contributing to the quantum amplitude. In fact, this determinant is dictated by the uncertainty principle for the conjugate variables such as coordinate and momentum. The merit of the average density valid for all paths, having the quantum spreading fixed by the initial distribution, is evident at the caustic and turning points. Here, the zeroth derivative $R_p(t;s,0) = 0$ provides for the concentration of the classical paths, for which the Van Vleck's determinats diverge.[28,29,31] However, our determinantal relation still remains to be a good solution for the quantum amplitude.

It is necessary to look more closely at the semiclassical recipe to gain insight about a frequency modulation of wave-packet correlations. The *S*-correlator is written as a trace of the polarization density matrix, see also eq 30,

$$S_{00}(t) = \mu^2\hbar^{-1}Tr\{\hat{\rho}(t)\} \propto \int_s \mathrm{d}r\, \mathrm{d}p\, \rho(s,t)$$

With initial condition $\hat{\rho}(0) = \hat{\rho}_0$, a solution formally satisfies to

$$\hat{\rho}(t) = \mathrm{e}^{-\mathrm{i}t\hat{H}_b/\hbar}\hat{\rho}_0\mathrm{e}^{\mathrm{i}t\hat{H}_x/\hbar} \tag{43}$$

The transport equation for the nondiagonal matrix element $\rho_{bx}(t)$ is immediately obtained with accuracy $\hbar^2$ to be sure containing the description of quantum interference on the Franck−Condon transition:

$$\frac{\partial\rho(s,t)}{\partial t} + \frac{p}{M}\frac{\partial\rho(s,t)}{\partial r} - \frac{\partial U_d(r)}{\partial r}\frac{\partial\rho(s,t)}{\partial p} - \frac{U_d(r)}{\mathrm{i}\hbar}\rho(s,t) = 0 \tag{44}$$

The difference potential $U_d(r) = U_b(r) - U_x(r)$ defines corresponding resonant frequencies. An average potential is the half sum of the molecular curves $U_a(r) = (U_b(r) + U_x(r))/2$. The equations of motion are

$$\dot{R} = P/M \qquad \dot{P} = -\partial U_a(R)/\partial R \tag{45}$$

So that, the *S*-correlations are represented as an integral of local density with fast oscillating exponential prefactor in the space *s* given by the expression,

$$Tr\{\hat{\rho}(t)\} = \int_s \mathrm{d}r\, \mathrm{d}p\, \mathrm{e}^{-\mathrm{i}\int_0^t \mathrm{d}\tau U_d(R(\tau;s,t))/\hbar}\rho_0(s(t)) \tag{46}$$

At the start, the function $\rho_0(s(0)) = \rho_0(R(0;s,0), P(0;s,0)$ has the quite simple shape of a Gaussian distribution. Its contour lines look like the stretched ellipses. Then, the map exhibits a complicated topology due to winding motion around a minimum of the average potential and its anharmonicity. Together with the fast oscillating functional for the difference potential of the B−X states, it presents a challenge to calculating the trace integral representation for 'topological singularities' of the turning point structure, which is common for the semiclassical approximations of wave mechanics.[31]

The solution to our problem is written down in Langrange coordinates $S = (R,P) = (R(0;s,t), P(0;s,t))$. By virtue of Liouville theorem, the phase volume in the jacobian transformation from Euler to Lagrange variables is invariant, while molecular potentials are independent of velocity. In the Langrange picture

$$Tr\{\hat{\rho}(t)\} = \int_S \mathrm{d}R\, \mathrm{d}P\, \mathrm{e}^{-\mathrm{i}\int_0^t \mathrm{d}\tau U_d(R(\tau;S,0))/\hbar}\rho_0(S) \tag{47}$$

the basic integrand becomes a function of *R*, *P*

$$\hat{\rho}(t) = \exp(-i\Phi(S,t))\rho_0(S)$$

To expand the path functional Φ in the exponent to the second order in departures from the point q_0, we use a series

$$\Phi(s,t) = \Phi^0 + \Phi^0_s(s - q_0) + {}^1/_2\Phi^0_{s,s_1}(s - q_0)(s_1 - q_0) + \ldots \tag{48}$$

where

$$\Phi^0 = \Phi(s_0,t) = \int_0^t \mathrm{d}\tau\, U_d(R(\tau;q_0,0))/\hbar$$

and the path $s_0(t) = (R(0; q_0, t), (P(0; q_0, t))$ obeys eq 45. By reusing the vector and matrix notation again, one can represent the final expression as a two-dimensional Gaussian integral

$$S(t) = (\mu/\hbar)^2(\det\hat{\Pi})^{-1/2}\exp\left(-i\Phi^0 - \frac{1}{4}\vec{U}\hat{\Pi}^{-1}\vec{U}^{\dagger}\right) \tag{49}$$

where the vector $\vec{U}$ and matrix Π are given by

$$\vec{U} = (\Phi^0_r, \Phi^0_p);$$
$$\hat{\Pi} = \begin{pmatrix} (\Delta R)^{-2} + i\,\Phi^0_{rr}/2, & \mathrm{i}\,\Phi^0_{rp} \\ i\,\Phi^0_{rp}, & (\Delta R/\hbar)^2 + \mathrm{i}\,\Phi^0_{pp}/2 \end{pmatrix} \tag{50}$$

The phase modulation is set by the function $\Phi^0(t)$. Additional corrections in the exponent are responsible also for the decay amplitude giving generalized Debye−Waller factors for wave-packet recoiling. The phase and amplitude formulas may be simplified due to peculiar features of molecular curves, short times evolution, etc. This approach would be of interest to address Landau−Ziner transitions, and the spectral lines structure from impact center to static wings may be uniformly exploited. An analytical formulation of the globally optimal fields has some advantage of being used to model the molecular wave-packet correlations. On propagating in a space the laser pulse might be tailormade to mimic the known optimal fields. With this aim the high frequency filtering in optical guides, nonlinear frequency dispersion, reflection from holographic film, gratings, etc. giving the right temporal and spectral trends may be adapted to perform the quantum control.

As an example, we will discuss a chirping in static wing of spectral molecular line. Accessed by the ultrashort pulse, the wave packet develops in the average potential $U_a(R)$ between points connected by the direct path. For a small τ (a femtosecond scale), these points are close together on the trajectory

$$R(\tau; R, P) = R + \tau P - (\tau^2/2M)\,(\mathrm{d}U_a/\mathrm{d}R)$$

The difference potential in eq 46 can be expanded for the small departures from the equilibrium point q_0, and we may rewrite the frequency in Φ^0 as a power series for a small τ

$$U_d(R(\tau; q_0, 0) = U_d(R_0) - (\tau^2/2M)\,(\mathrm{d}U_a/\mathrm{d}R_0)(\mathrm{d}U_d/\mathrm{d}R_0) =$$
$$= U_d(R_0) - (\tau^2/4M)\,(\mathrm{d}U_b/\mathrm{d}R_0)^2$$

Since the condition $\mathrm{d}U_x(R)/\mathrm{d}R = 0$ (zero force) should be met in $R = R_0$ (at a minimum of X curve), the result is the quadratic chirp lowering the pulse frequency with a correction coefficient of 0.25 to its classical rate in eq 34. The correction of this sort is not surprising for the classical−semiclassical−quantum correspondence. Moreover, considering more closely the phase and amplitude modulation of wave packet correlations resulted from $\vec{U}\hat{\Pi}^{-1}\vec{U}^{\dagger}$ in eq 49, one can find additional corrections due

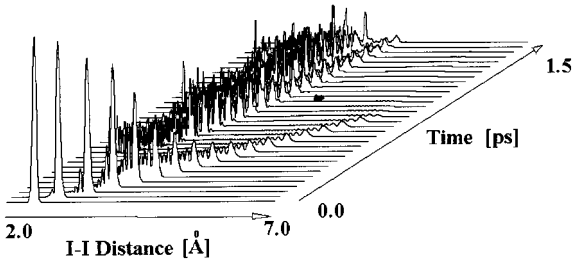

Figure 2. The picture shows the nodal structure of bound wave packet ranging between 2.2−4 Å. The wave packet fringes are due to interference of the wave packet in virtue of multiple collisions against the molecular curves.

to recoil from the slope molecular curve. The first nonvanishing terms of the power τ and τ^3 in the exponent are an exact match the quantum formulas in the Condon model (see section II after eq 16). It is worth stressing that the wave packet is found in the coherent superposition of two resonance states (i.e., B and X, and their mixing will reduce the chirp rate on the classically gained formula in eq 34) because the molecular force acts only through the curve B (in recoiling from the inner curve), and does not in the equilibrium point of curve X.

This argumentation must be revised further for returning trajectories on a long time duration. In the case, our uniform treatment warrants a more careful study that will be reported elsewhere. For completeness sake, the basic ideas of quantum control should be examined in a quantum simulation, which is favored to the semiclassical treatment, if one cannot limit by one classical path. Thus, in the next section, we shall rely on the quantum computation leaving aside a detailed numerical analysis of the classical equations.

4. Numerical Simulations

The quantum model eq 3 for the motion along one active I−I coordinate and electronic transition belongs to the polynomial class of numerical complexity of N linear equations, where N is the number of grid points. There is more than one recipe with which to perform their computations.[32] The QR diagonalization requires the $O(N^3)$ operations. In specific cases, the QR algorithm, as a stable spectral decomposition, can be used for the wave-packet propagation. The time implicit symmetrical schemes of Gaussian elimination[33] necessitate $O(N)$ operations. The symmetrized split operator method does $O(N\log(N))$ steps based on the fast Fourier transform (FFT).[34] The FFT propagates the wave packet similar to Feynman's path integral and alternates the coordinate and momentum representations involving the thorough dynamical picture in hand. These methods are in good agreement. The practical value of FFTs or Gaussian elimination is that they enable to get rid of the matrix diagonalization.

The absorbing boundary condition has been used in the numerical simulations. The imaginary negative optical potential discriminates the outgoing wave packet at outer edge of the numerical grid and has no effect on the bound states. This feature is visible in Figure 2, where the molecular dynamics following impact resonance interaction on B−X transition is shown. The ground state replica transforms into a wave packet which is scattering above the molecular dissociation limit and binding below it. The scattering states, shown in the foreground of Figure 2, are involved due to impact photodissociation (i.e., the δ-like pulse action). This branch is not mixed with the bound-bound transitions responsible for coherent recurrences, while the wave packet recoils against the molecular walls and oscillates spreading for the B state anharmonicity.

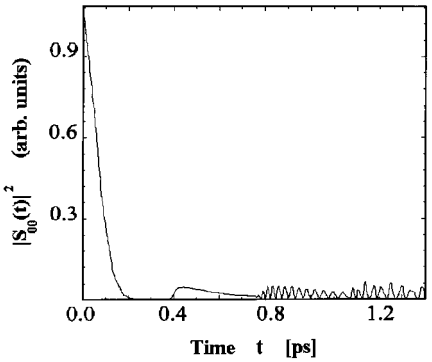

Figure 3. Intensity of fundamental overtone of resonant scattering as a function of time. This resonance transition is induced by the photon impact (the δ-like pulse). The scattering B states contribute to monotonic free decay signal first few fs. The bound states interference, present in the background in Figure 2, is responsible for reviving the resonance Raman scattering after 320 fs delay, which is matched with a molecular period (at 570 nm in B state).

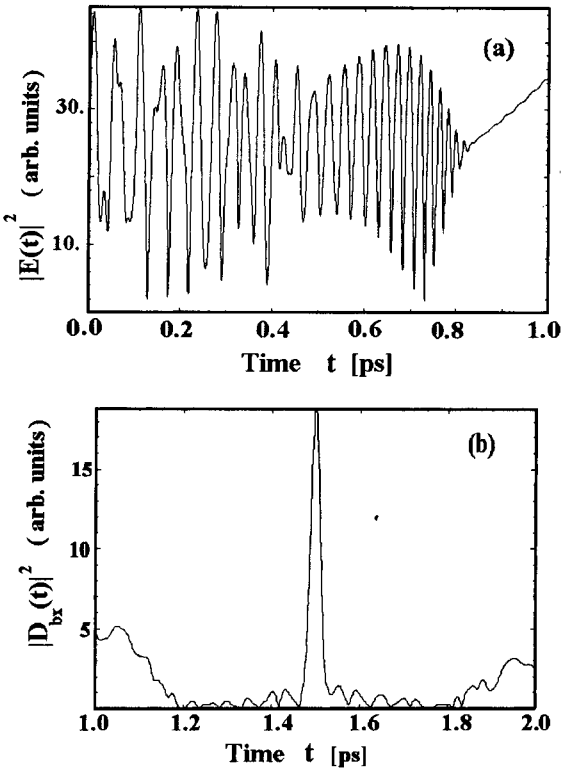

Figure 4. The square 1 ps gate of the optimal field in a. This optimal field creates the dipole transition moment shown in b. The accomplishment of our coherent objective is evident at target time equal to 1.5 ps.

The resonance scattering radiation in the wake of ultrashort pulse proceeds in two stages: a fast monotonic decay due to direct photodissociation gives way to a "nonregular" reviving. This picture is shown in Figure 3 for the fundamental overtone of Raman intensity. Since a damping out is assumed to be small, the wave packet correlations hold during many molecular periods. The amplitude and phase profile will follow in reverse order. Thus, Figure 3 showing its fundamental overtone intensity must be read " from right to left". The phase conjugate scattering signal in Figure 4a has been designed to drive the spread waves toward t_d. The target time t_d exactly represents the starting point of wave-packet correlations. Furthermore, on

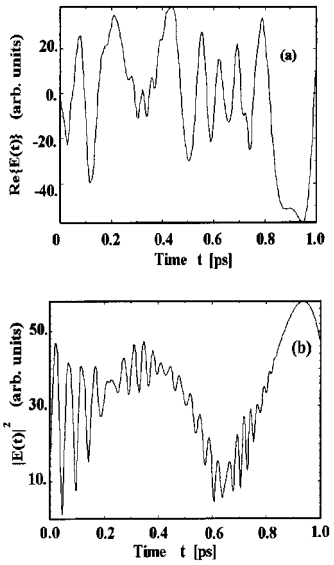

Figure 5. The intensity of optimal field in a and its real part in b. This optical pulse is designed to create 50 fs square gate optical coherence at target time 1.5 ps.

going back in time their envelope $S(t_d - \tau)$ is not δ correlating as a white noise signal.

There are two regular trends: the negative frequency chirp, which has been explained with the semiclassical arguments, and amplitude growing to the pulse end. The last feature stemmed from the reversibility theorem can be also understood qualitatively. Since the wave packet is spreading between turning points, the result is a small amplitude almost everywhere in the classically accessible Franck−Condon region. The optimal field on its start is set by a projection of the spread wave packet to the X state. The *S*-correlations undergo fast oscillations due to multiple recoils of the wave packet against molecular walls and its spreading accompanied by decreasing amplitude. Evolving back in time, the wave packet becomes more regular and its shape is recovered and copies well localized replica of the ground X state. Focusing the wave packet in the vicinity of the inner turning point results in a further rise of its amplitude.[49] The projection to the ground X state grows together. This explains why the globally optimal field behaves in such a way in Figure 4a. Induced resonance transient given by eq 4 is shown in Figure 4b. The 1 ps square gate of optimal field creates the transient spike at delay time 1.5 ps. The temporal full width at half maximum (fwhm) equals $T_w = 25$ fs that is in good agreement with the kinematical overlap lifetime $\tau_{rec} = 15$ fs.

This semiclassical estimate is astonishingly accurate although less than quantum computed. There are two main reasons of this distinction. The wave-packet interference is absent in the classical kinematics and the dispersion of excited state is not taken into account. Thus, the ignorance of quantum wave nature underestimates the width of the coherent peak. To cure the situation, the semiclassical uniform approach, which copes with initial quantum distribution, classical motions, caustic and turning points, may be applied.

For definiteness sake, setting $T_g = 50$ fs square gate of optical target *G* at the delay time 1.5 ps, we now can consider a realistic optical transient. Averaging the globally optimal envelope over *G* washes out the high frequency components as shown in Figure 5. However, the average pulse shape is yet endowed with a chirp. This feature is exhibited in Figure 6 a, where Wigner

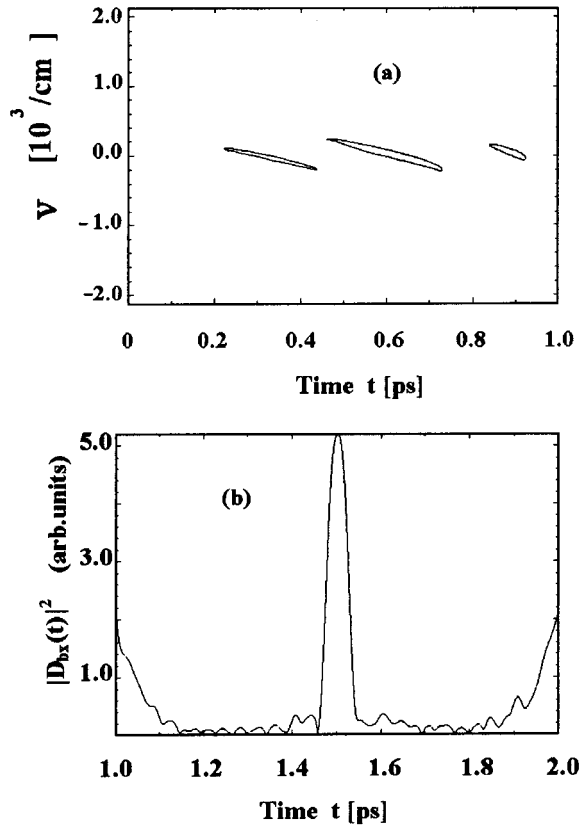

Figure 6. The frequency−time plot of the globally optimal pulse for the 50 fs square gate target is given by the contour map at half a maximum of Wigner spectrogram in a. The coherent transient in b is created by the optimal field. The temporal fwhm equal to 60 fs fits well the 50 fs square gate target.

spectrogram is shown. The Wigner function of the optimal fields is defined as

$$W(t,\nu) = \int \frac{d\tau}{2\pi\hbar} e^{i\nu\tau/\hbar} E\left(t + \frac{\tau}{2}\right)^* E\left(t - \frac{\tau}{2}\right)$$

Picosecond square gate envelope and periodic boundary condition have been used in evaluating the spectrograms. The frequency-time maps manifest a striking correlation between the optimal fields and wave-packet evolution. For instance, the envelop of allocated duration $T_p = 1$ ps consists of more shorten subpulses. Their number is associated with the number of vibrational cycles between turning points during T_p. For every recoiling from inner molecular core the wave packet gives rise to a subpulse. The contour levels of the two-dimensional Wigner spectrogram are taken at one-half a maximum height. A slope and concavity characterizes respectively a linear and quadratic frequency chirp of subpulse. The semiclassical reasoning relate the chirping to wave packet velocity and acceleration. The chirp is in fact linear because time duration of pulse T_p (in picosecond range) is much more than the recoil lifetime $\tau_{rec} = 15$ fs. Thus, the wave packet is far from turning points and does not accelerate most of the time. The spectral fwhm in Figure 6a is about $\Delta\nu \approx 500$ cm^{-1}, being consistent with the reciprocity relation $\Delta\nu = 2\pi\hbar/\Delta T_g$.[35]

A minor decoherence of the objective as shown in Figure 6b is obtained in our numerical simulation. The temporal fwhm is about 60 fs being 10 fs over the square gate target width $T_g = 50$ fs. The distinction stems from the wave packets quantum dispersion. The wave packet dynamics is displayed in Figures 7 and 8. The resonance frequency is 19050 cm^{-1} above the

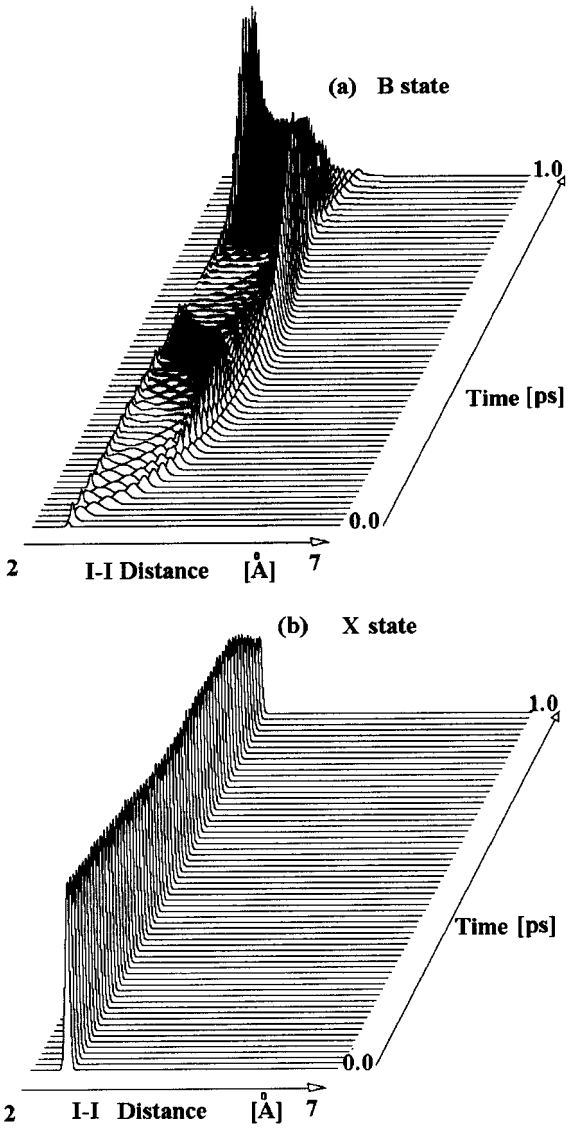

Figure 7. The tailored field shown in Figure 5 excites the delocalized vibrational wave packet in a. The X state in b holds its initial spike shape centered at 2.66 Å with variance 0.05 Å.

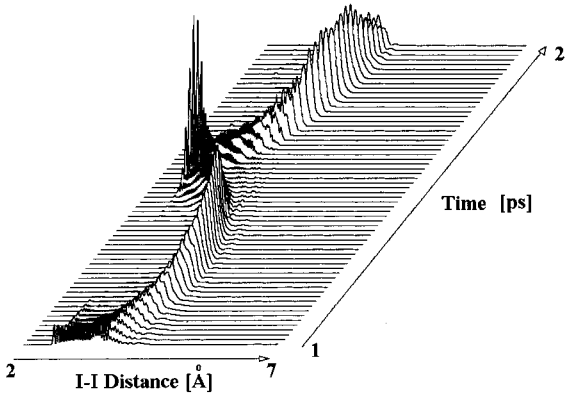

Figure 8. The wave packet B free propagates after the pulse to a tightly squeezed state at the inner turning point to overlap well the ground-state X at target time 1.5 ps.

ground X term; the excitation bandwidth is about 500 cm^{-1} (fwhm). Thus, the wave packet B is created below the molecular continuum to spread from 2.2 to 4 Å not far from its dissociation limit. Given intensity of transitions, the depopulation of state X is involved to the pulse end, although the X state localization is not affected at the saturation. The optical transient rises and falls, following the wave packet recoils from the inner core. The spatial variance of a maximum focused wave packet at target time reaches 0.04 Å, being slightly less than the original localization in agreement with our qualitative reasoning. The result is robust to slow sinusoidal or gaussian aberrations of optimal fields and akin to known stability of phase conjugate fields due to the wave speckle structure.[36]

5. Conclusion and Future Perspectives

The numerous possible applications in femtosecond spectroscopy are rested on the concept of coherence. The proceedings of Femtochemistry III Conference in Lund testify (see the special issue of the *Journal of Physical Chemistry*), that this realm of knowledge is flourishing and another lines of researches have now been opened. As an example we refer the field of deemed quantum computers.[37−39] Here, controllable coherence of logic gates could boost performance of massive parallel computation exponentially with number of quantum nodes. These nodes may be constituted from clusters or single molecules and their resonance optical transitions must act in concert with vibrational wave packets captured by "molecular cavities". A run stage of a quantum computer, its coherence may not be affected by environment.[40] Thus, the danger of dephasing requires the optical coherence to be actively controlled according to a state-mapping protocol. From this point of view, the reversibility theorem stated in our paper exemplifies a paradigm of controllability expected for wave packets dynamics and optical transients. In fact, the fundamental connection between physical laws and computations based on time reversable Hamiltonians has been addressed yet by R. Feynman.[41] The computational quantum networks requires the reversable transmission among distant nodes.[42]

The central aim of this paper is to set a globally optimal solution to a maximum squeezing the optical coherence of a single molecule. The sufficient conditions of recovering coherence have been stated in the reversibility theorem. Our time reversed fields have been tested in the model computation of I_2 B−X transition confirming effeciency of the phase conjugate resonant Raman scattering for quantum control. The result is not limited only to diatomic molecules in gas or condensed states, but is valid for the quantum control of electron wave packets as well.[43,44]

The four-wave mixing interaction and related stimulated Raman emission is deserving of mention. These optical transients would make it possible to automate the quantum control to be held both for bound states and molecular continuum. To take one example, ultrashort transform limited pulses driving bound-free transitions result in the photon echo of photodissociation,[45] to mean an automated controlling wave packet motion. Photon echoes[19] imply that dynamical holograms are written on resonance Franck−Condon transitions. But it takes more strong laser fields to induce at least the third-order nonlinear polarization. A self-adaptive "quantum mirror" has been devised[36,46] to reverse wave evolution on curing the optical aberrations of a noise wave front propagated trough inhomogenious media. Moreover we have seen that the phase cojugate (time-reverse) Raman scattering negates also delocalization of molecular wave packets.

The use of the phase conjugate signals presents an intriguing illustration of how the original quantum state is restored in the matter−wave interferometry. An uniform semiclassical formula has been derived for the optimal field envelop. The simple estimates are contrasted with quantum simulation. We conclude

that femtosecond coherence of a single molecule must exist in varied conditions (even on resonant transitions saturated to the pulse end). Robustness of our molecular magnetron design has been demonstrated also. We propose to test experimentally the molecular magnetron design verifying the quantum holography directly on observing delayed sparks of femtosecond fluorescence which is excited by a more long picosecond pulse in optically thin sample.

Acknowledgment. We thank K. R. Wilson for reprints on controlling the future of matter available before their publication. The work benefited from useful discussions with S. R. Hartmann, J. Jortner, M. Chergui, and I. Averbukh. Sincere thanks to the referees of our manuscript for their critical reading, advice, and editorial help in getting the paper to readable form. One of the authors (A. Rudavets) is especially indebted to V. Aquilanti, B. Soep, J. Chergui, K. Kulander, and V. Sundstroem for a kind hospitality extended to him to visit quantum control meetings around the world. It was supported by the Russian Foundation for Basic Researches Grant 96-02-18760.

References and Notes

(1) Pierce, A. P.; Dahleh, M. A.; Rabitz, H. *Phys. Rev. A* **1988**, *37*, 4950. Warren, W. S.; Rabitz, H.; Dahleh, M. *Science* **1993**, *259*, 1581.

(2) Shapiro, M.; Brumer, P. *Chem. Phys. Lett.* **1993**, *208*, 193.

(3) Averbukh, I. S.; Shapiro, M. *Phys. Rev.* **1993**, *A47*, 5086. Abrashkevich, D. G.; Averbukh, I. S.; Shapiro, M. *J. Chem. Phys.* **1995**, *101*, 9295.

(4) Yeazell, J. A.; Stroud, C. R., Jr. *Phys. Rev. Lett.* **1988**, *60*, 1497. West, J. A.; Stroud, C. R., Jr. *Optics Exprs*. **1997**, *1*, 31.

(5) Krause, J. L.; Whitnell, R. M.; Wilson, K. R.; Yan, Y.; Mukamel, S. *J. Chem. Phys.* **1993**, *99*, 6562.

(6) Kohler, B.; Yakovlev, V. V.; Che, J.; Krause, J. L.; Messina, M.; Wilson, K. R.; Whitnell, R.; Yan, Y. *Phys. Rev. Lett*. **1995**, *74*, 3360.

(7) Dubov, V.; Rabits, H. *J. Chem. Phys*. **1995**, *103*, 8412.

(8) Apkarian, V. A. In *Ultrafast Physical and Chemical Processes in Molecular Systems, Proceedings of Femtochemistry: The Lausanne Conference*; Chergui, M., Ed.; 1995; p 603.

(9) Bardeen, C. J.; Che, J.; Wilson, K. R.; Yakovlev, V. V.; Apkarian, V. A.; Martens, C. C.; Zadoyan, R.; Kohler, B.; Messina, M. *J. Chem. Phys.* **1997**, *106*, 8486.

(10) Zewail, A. H. *Ultrafast Physical and Chemical Processes in Molecular Systems, Proceedings of Femtochemistry: The Lausanne Conference*, Chergui, M., Ed.; 1995; p 3.

(11) Jortner, J. *Ultrafast Physical and Chemical Processes in Molecular Systems, Proceedings of Femtochemistry: The Lausanne Conference*; Chergui, M., Ed.; 1995; p 15.

(12) Tannor, D. J.; Rice, S. A. *J. Chem. Phys*. **1985**, *83*, 5013.

(13) Kosloff, R.; Rice, S. A.; Gaspard, P.; Tersigni, S.; Tannor, D. *J. Chem. Phys.* **1989**, *139*, 201.

(14) Scherer, N. F.; Carlson, R. J.; Matro, A.; Du, M.; Ruggiero, A. J.; Romero-Rochin, V.; Cina, J. A.; Fleming, G. R.; Rice, S. A. *J. Chem. Phys.* **1991**, *95*, 1487.

(15) Milliken, R. S. *J. Chem. Phys.* **1971**, *55*, 288.

(16) Gruebele, M.; Zewail, A. H. *J. Chem. Phys.* **1992**, *98*, 883.

(17) Xu, J.; Schwenter, N.; Henning, S.; Chergui, M. *J. Chem. Phys*. **1994**, *101*, 7381; *J. Chim. Phys.* **1995**, *92*, 541.

(18) Landsberg, G.; Mandelstam, L. *Z. Phys.* **1930**, *60*, 364. Mandelstam, L.; Landsberg, G.; Leontowitsch, M. *Z. Phys.* **1930**, *60*, 334. Tamm, I. *Z. Phys.* **1930**, *60*, 345.

(19) Friedberg R.; Hartmann, S. R. *Phys. Rev.* **1993**, *48*, 1446.

(20) Tellinghuisen, J. *J. Chem. Phys.* **1973**, *58*, 2821; *J. Chem. Phys.* **1982**, *76*, 4736.

(21) Heller, E. J. *Chem. Phys.* **1978**, *68*, 2066.

(22) Schkurinov, A. P. Private communication.

(23) Cerrulo, G.; Bardeen, C. J.; Wang, Q.; Shank, C. V. *Opt. Lett*. **1996**, *19*, 737.

(24) Cao, J.; Bardeen, C. J.; Wilson, K. R. *Phys. Rev. Lett*. **1997**. Submitted for publication.

(25) Baumert, G. T.; Grosser, M.; Thalweiser R.; Gerber, G. *Phys. Rev. Lett.* **1991**, *67*, 3753.

(26) Weiner, A. M.; Leaird, D. E.; Patel, J. S.; Wullert, J. L. *Opt. Lett.* **1990**, *15*, 326. Wefers, M.; Nelson, K.; Weiner, A. M. *Opt. Lett.* **1996**, *21*, 746.

(27) Hillegas, S. W.; Tull, J. X.; Goswami, D.; Strickland, D.; Warren, W. S. *Opt. Lett.* **1994**, *19*, 737.

(28) Dirac, P. A. M. *The Principles of Quantum Mechanics*; Oxford: Claredon Press: New York, 1947.

(29) Cao, J.; Wilson, K. R. *J. Chem. Phys.* **1997**, *107*, 1441.

(30) Landau, L. D. *Phys. Z. Sowjetunion* **1932**, *1*, 88; *Phys. Z. Sowjetunion* **1932**, *2*, 46.

(31) Berry, M. V.; Mount, K. E. *Rep. Prog. Phys.* **1972**, *35*, 315.

(32) Press: W. H.; Teukolsky, S. A.; Vetterling, W. T.; Flannery, B. P. *Numerical Recipes in Fortran*, The art of Scientific Computing, 2nd ed.; Cambridge University Press: Cambridge, 1992.

(33) Fedorenko R., Introduction into Computational Physics; Moscow Institute of Physics and Technology Publishing; Moscow, 1994.

(34) Feit, M. D.; Fleck, J. A., Jr.; Steiger, A. J. *Comput. Phys.* **1982**, *47*, 412.

(35) S. R. Hartmann suggested that a noisy emission may be transformed into ultrafast optical signal of equivalent bandwidth (private communication to A. R.).

(36) Zeldovich, B. Ya.; Pilipetsky, N. F.; Schkunov, V. V. *Phase Conjugated Wave Fronts*; Nauka: Moscow, 1985. Ragulsky, V. V. *Optical Phase Conjugaion by Stimulated Scattering*; Nauka, Moscow: 1990.

(37) Feynman, R. P. *Found. Phys*. **1986**, *16*, 507.

(38) Duetsch, D. *Proc. R. Soc., London* **1989**, *A425*, 73.

(39) Lloyd, S. *Sci. Am.* **1995**, *273*, 140.

(40) Unruh, W. G. *Phys. Rev.* **1995**, *41*, 992.

(41) Feynman, R. P. *Int. J. Theor. Phys.* **1982**, *21*, 467.

(42) Cirac, J.; Zoller, P.; Kimble, H. J.; Mabuchi, M. Quantum State Transfer and Entaglement Distribution among Distant nodes in Quantum Network, quant-ph/9611017.

(43) Schafer, K. J.; Krause, J. L. *Opt. Exp.* **1997**, *1*, 210.

(44) Noel, M. W.; Stroud, C. R., Jr. *Opt. Exp*. **1997**, *1*, 176.

(45) Akulin, V. M.; Dubovitskii, V. A.; Dykhne, A. M.; Rudavets, A. G. In Ultrafast Physical and Chemical Processes in Molecular Systems, Proceedings of Femtochemistry: The Lausanne Conference; Chergui, M., Ed.; 1995; p 62.

(46) Pepper, D. M. *Opt. Eng.* **1982**, *21*, 156.

(47) J. Jortner has drawn our attention to curve-crossing effects in experiments reported by V. Apkarian[8] et al. and M. Chergui[17] et al. Our theory can be extended for B−(B″,a,a′) couplings affecting the quantum control. The results is the entanglement with continuum molecular states shortening optical transients.

(48) It is worth noting that a central role of the classical trajectories for calculating matrix elements of high excited states has been well-known since the 1930s, due to Landau seminal contribution to the chemical collisions theory.[30]

(49) A clear analogy is given by a point of intense radiation behind burning-glass exposed to sun.